Current Microbiology (2026) 83:201
https://doi.org/10.1007/s00284-026-04783-8

ORIGINAL PAPER

Surface Layer-Associated Protein on Nanoparticles from *Lactobacillus helveticus* Enhances the Response to LPS in RAW264.7 Cells

Chika Yamamoto[1] · Nao Fujiwara[1] · Ika Adhani Sholihah[2] · Mana Yamamoto[1] · Rinka Kizaki[1] · Daichi Ito[1] · Chinatsu Yokoi[1] · Saho Furukawa[1] · Hiroko Koyama[1] · Yoko Hirata[3] · Kyoji Furuta[4] · Hiroshi Takemori[1]

Received: 27 May 2025 / Accepted: 4 February 2026

Abstract
Lactic acid bacteria that persist in the gastrointestinal tract contribute not only to nutrient metabolism but also to the regulation of immune responses. Accordingly, these microorganisms and their components are classified as probiotics when administered in adequate amounts and shown to confer health benefits on the host. However, the mechanisms by which they interact with host cells remain poorly understood. Extracellular vesicles (EVs) have been shown to modulate functions in recipient cells, including both mammalian cells and microorganisms. Surface-layer associated proteins (SLAPs) are preferentially produced by Gram-positive syntrophic bacteria and are secreted to associate with the cell envelope. The dysfunction of SLAPs leads to disruption of the cell envelope, cell division, and cell–cell communication. In this study, we identified SLAP in extracellular vesicle-like nanoparticles (EV-LNPs) derived from *Lactobacillus helveticus* strain GIF001 (closed to strain VHProbi Y21) and observed enhanced immune responses—including nitric oxide and interleukin-6 production—in RAW264.7 cells when SLAP was added to the culture medium, either in the form of EV-LNPs or as a purified protein. Notably, *L. helveticus* EV-LNPs were internalized within 3 h and enhanced NF-κB signaling in response to lipopolysaccharide. Intracellular overexpression of SLAP led to increased activity of the inducible nitric oxide synthase promoter about 1.5 times, whereas deletion of the SLAP domain abolished this enhancement. Incubation of RAW264.7 cells with EV-LNPs or SLAP enhanced the uptake of *Escherichia coli*. These results suggest that EV-LNPs from *L. helveticus* may upregulate immune responses by activating host cell communication via SLAP.

Keywords S-layer associated protein · Lactic acid bacteria · Extracellular vesicles · Immune responses · Removal of *E. coli*

Introduction

Extracellular vesicles (EVs) are nanovesicles secreted by living cells, including not only animals but also plants and microorganisms [1, 2]. Lipid bilayers, together with membrane proteins, form the envelope of EVs, while the lumen contains proteins and nucleic acids, such as DNA and RNA [3]. These substances play important roles in intercellular communication and, in some cases, interorganismal communication, particularly in modulating host responses. For example, such interactions have been observed between cancer cells and the immune system, as well as between symbiotic bacteria and the host immune system, where Toll-like receptor (TLR) signaling can lead to immune checkpoint inactivation [2]. However, the precise characteristics of these interactions remain largely unknown.

✉ Hiroshi Takemori
takemori.hiroshi.r7@f.gifu-u.ac.jp

[1] Department of Chemistry and Biomolecular Science, Faculty of Engineering, Gifu University, Yanagido 1-1, Gifu 501-1193, Japan

[2] United Graduate School of Drug Discovery and Medical Information Sciences, Gifu University, Gifu 501-1193, Japan

[3] Life Science Research Center, Institute for Advanced Study, Gifu University, Gifu 501-1193, Japan

[4] Gifu Exosome Co., Ltd, Yabuta-minami, Gifu 500-8384, Japan

Published online: 21 February 2026

In microorganisms, EVs-like nanoparticles (EV-LNPs) are formed from outer membrane components or intracellular vesicles. One such structural component is the surface layer (S-layer), a cell wall-associated structure composed of a two-dimensional array of proteins or glycoproteins that constitutes the outermost layer of the cell envelope in many bacteria and nearly all archaea [4]. In Gram-positive bacteria, such as lactic acid bacteria, the S-layer is attached to the underlying peptidoglycan layer, whereas in Gram-negative bacteria, such as *Escherichia coli*, it is associated with the outer membrane or the lipopolysaccharide (LPS) layer [5]. These components are essential for maintaining cell structure and cell division, and also function as bioactive complexes recognized by host cells.

S-layer associated protein (SLAP), also known as S-layer protein (SLP), is a membrane-associated protein that preferentially targets peptidoglycan [6]. SLAPs are characteristic features of symbiotic bacteria, such as lactic acid bacteria, and are recognized as supporting factors for membrane integrity and defense systems through interorganismal communication [5, 7, 8]. Dysfunction of SLAPs is believed to disrupt the regulation of the microbiota, leading to pathological conditions in the host. Most SLAPs possess a repeated structure in the C-terminal region, known as the SLAP domain, which has been found to bind to the S-layer.

In this study, we identified SLAP in EV-LNPs derived from *Lactobacillus helveticus* strain GIF001 (a strain closely related to strain VHProbi Y21, with a 100% genomic sequence match for the *slap* gene). The addition of EV-LNPs, purified SLAP, or intracellular overexpression of SLAP in RAW264.7 mouse macrophages/monocytes led to the activation of immune signaling pathways and uptake of *E. coli*, suggesting an evolutionarily conserved mechanism for communication between symbiotic bacteria and host cells.

Materials and Methods

Purification and Analysis of EV-LNPs

Lactic acid bacteria (*L. helveticus*, *L. casei*, *L. paracasei*, *L. acidophilus*, *Streptococcus thermophilus*) were isolated using MRS agar plates (Biokar Diagnostics, Paris, France) from a commercially available KEFIR supplement (Laby Lab, Tokyo, Japan) and yogurt produced by Takasu farmers (Gifu, Japan). Because *L. delbrueckii* often replaces *S. thermophilus* during culture, we used an isolated strain, *L. delbrueckii* srain NBRC 3202, obtained from a bank of National Institute of Technology and Evaluation (Tokyo, Japan). Each strain was identified by amplification of 16S ribosomal RNA genes using polymerase chain reaction (PCR) with the primers 5'-AGAGTTTGATC(A/C) TGG CTCAG and 5'-CCGTCAATTC(A/C)TTTGAGTTT. To obtain a longer 16 S ribosomal RNA gene sequence of *L. helveticus*, an additional reverse primer (5′-GCTTCGTGC AGTCGAGTTGCA) was designed. The results are shown in Table S1. The 16 S ribosomal RNA gene sequence of *L. helveticus* used in this study (strain GIF001) was deposited in the GenBank database under the accession number LC907079.2.

The procedure for EV-LNPs purification is described in [9–11]. Briefly, a bacterial colony was suspended in 25 mL of MRS broth and incubated under anaerobic conditions at 33 °C for 24 h with stirring. Then, a 5 mL aliquot was transferred into 100 mL of fresh MRS broth and further incubated for an additional 24 h without pH adjustment.

The supernatant (50 mL) was collected by centrifugation at 8,000 × g for 30 min and subsequently filtered using 75-mm bottle-top filters made of polyether sulfone (PES) with pore sizes of 0.45 µm (Merck, Darmstadt, Germany). The filtrate was subsequently passed through a 0.1 µm PES filter (Merck), and EV-LNPs in the 0.1 µm-filtrate were captured on a polycarbonate track-etched (PCTE) membrane filter (47 mm, 0.05 µm pore size; GVS Germany GmbH, Sinzig, Germany) and washed twice with 2 mL of phosphate-buffered saline (PBS). EV-LNPs were recovered using 2.5 mL of PBS (20-fold concentration), followed by sterilization through a 0.2 µm PES syringe filter (GVS). To prepare the EV-LNP–depleted fraction, the 0.05-µm flow-through fraction was further concentrated using a 30-kDa PES spin column (Pall Corp., Port Washington, NY, USA).

Protein concentration was measured with Protein assay kit (Nacalai Tesque, Kyoto, Japan). EV-LNPs were labeled with GIF-2276 and the ExoSparkler Exosome Membrane Labeling Kit-Red (Exo-SP) from Dojindo (Kumamoto, Japan), as described by [9, 10], and separated using a size-exclusion chromatography (SEC) column, TSKgel G6000PW (TOSOH, Tokyo, Japan). Fluorescent signals were detected using tandemly linked detectors, RF-10 A XL (Shimadzu, Kyoto, Japan). Average size and concentration of EV-LNPs were measured by dynamic light scattering (DLS) analysis using the Zetasizer Nano (Malvern Panalytical, Westborough, MA, USA). The particle number (concentration) was calculated using the information provided for the standard particles, deep-blue–dyed latex beads with a diameter of 240 nm (Merck) (Fig. S1 A and B). The well-purified EV-LNP fractions contained approximately 7×10^{10} particles/mL, corresponding to about 0.5 mg/mL of protein. We also prepared two independent SLAP fractions, for which the purification methods are described in the following section. These independently prepared EV-LNP and SLAP fractions yielded almost identical results.

The morphological structure of the EV-LNPs was observed by the transmission electron microscope (TEM) JEM-2100 (JEOL, Tokyo, Japan).

SLAP Purification and Overexpression

To identify protein markers in EV-LNPs, the EV-LNP fraction was mixed with an equal volume of 3 × sodium dodecyl sulfate (SDS) sample buffer supplemented with 10% 2-mercaptoethanol (Fujifilm Wako, Osaka, Japan), denatured, and separated by SDS–polyacrylamide gel electrophoresis (SDS-PAGE). Following staining with Coomassie Brilliant Blue R-250 (Nacalai Tesque, Kyoto, Japan), visible protein bands were excised and subjected to proteomic analysis (Nippon Proteiomix Inc., Miyagi, Japan).

The DNA sequence of the *slap* gene from *L. helveticus* used in the present study was deposited in the GenBank database under the accession number LC907080.1. The preparation of rabbit antibodies against the C-terminal 15 amino acids of *L. helveticus* SLAP was outsourced to Sigma-Aldrich Japan (Hokkaido, Japan) and purified with protein A agarose (Merck). Because the PCR-amplified SLAP gene from *L. helveticus* was not suitable for the overexpression in mammalian cells, a codon-optimized SLAP DNA for human cells was synthesized by GenScript (Piscataway, NJ, USA) and cloned into the *Bam HI–Not I* site of the pcDNA3.1 vector (DNA sequence shown in Fig. S2).

To generate the ΔSLAP mutant by site-directed mutagenesis, a stop codon was introduced into the coding region upstream of the SLAP domain using the oligonucleotides 5'-GGTACCTCTGTTGCC*TAGG*CCATCATGCACAACG and its complement (The underlined nucleotides are substitutions that create the *BlnI* restriction site.). To delete the N-terminal region, the oligonucleotides 5'-CACAGTGGTACCTCTG*GATCCA*TGACCATCATGCACAACG and its complement were used (the underlined nucleotides are substitutions that create the *BamHI* restriction site). The cDNA fragment encoding the N-terminal region was removed by *BamHI* digestion followed by self-ligation.

To purify SLAP from the bacterial membrane, approximately 2 g of *L. helveticus* cells were suspended in 20 mL of ice-cold 2 M LiCl for 30 min, as described in [12]. The LiCl extract was recovered by centrifugation at 8,000 × g for 30 min, dialyzed against PBS, and concentrated to 1 mL using the 30 kDa Vivaspin 2 PES concentrator (Sartorius, Göttingen, Germany).

Cell Assay

RAW264.7 cells were obtained from the American Type Culture Collection (VA, USA) and maintained in RPMI medium supplemented with 10% heat-inactivated fetal calf serum (FCS) and a penicillin–streptomycin mixture (Fujifilm Wako, Osaka, Japan). HEK293A cells (Thermo Fisher Scientific, MA, USA) were maintained in Dulbecco's Modified Eagle Medium. To evaluate NO and IL-6 / TNFα production, RAW264.7 cells (1×10^4 cells/well) were seeded in a 96-well plate. After 18 h of incubation, various concentrations of EV-LNPs or purified SLAP were added to the wells, followed by incubation with or without 0.5 μg/mL of LPS (Fujifilm Wako: Catalog No. 128–05171) for an additional 24 h. Subsequently, to measure NO, 100 μL of the supernatant was mixed with 100 μL of Griess reagent [1% sulfanilamide, 0.1% N-(1-naphthyl)ethylenediamine, and 0.625% (w/v) phosphoric acid; Merck] and incubated for 20 min at room temperature [13]. To quantify IL-6 and TNFα, a mouse IL-6 or TNFα enzyme-linked immunosorbent assay (ELISA) kit was purchased from BioLegend (San Diego, CA, USA). Anti-iNOS antibody (GTX130246), and anti-NF-kB (GTX102090), anti-p38 (GTX110720), and anti-pp38 (GTX133460) were purchased from GeneTex (Irvine, CA, USA). Anti-GAPDH antibody (M171-7) was from MBL Co. ltd. (Nagano, Japan).

For reporter assay, RAW264.7 cells (3×10^4 cells/well) were seeded in a 24-well plate 12 h prior to plasmid transformation. The inducible nitric oxide synthase (iNOS) promoter–firefly luciferase reporter plasmid has been described previously [14]. The AP-1 (pTA-AP1) and NF-κB (pTA-NF-κB) firefly luciferase reporter plasmids were purchased from Takara Bio (Kyoto, Japan). These firefly luciferase reporters (100 ng/well) were co-transfected with 100 ng/well of *Renilla* luciferase plasmid (pRL-TK; Promega, Madison, WI, USA), for normalization of transformation efficiency, using PEI-Max reagent (Funakoshi, Tokyo, Japan) (plasmid DNA : PEI-Max = 200 ng : 1 μL/well). Luciferase activities were measured using the Dual-Luciferase Reporter Assay System (Promega).

For *E. coli* incorporation assay, RAW264.7 cells (1×10^4 cells/dish: Azuone, Tokyo, Japan) were used. EV-LNPs (containing 10 μg of protein) were incubated with 200 μM GIF-2276 at room temperature for 8 h, and unreacted GIF-2276 was removed using a 300 kDa PES spin column (Pall) at 3000 g for 20 min. The labeled EV-LNPs were resuspended in 100 μL of PBS, and 10 μL of the suspension was added to the culture medium of RAW264.7 cells with lysosomes pre-labeled using 1 μM of LysoBright™ Red (ATT Bioquest, Pleasanton, CA, USA) for 20 min. During incubation with the labeled EV-LNPs, the FCS concentration was reduced to 1%, while antibiotics were continuously supplied.

The *E. coli* uptake assay was conducted based on a previous report [15]. Briefly, *E. coli* (JM109) was transformed with the mCherry expression plasmid pTarget-mCherry [16], and cultured overnight in LB medium supplemented

with 1 mM Isopropyl β-D-1-thiogalactopyranoside (Fujifilm Wako). Bacteria numbers were determined using LB agar plates and adjusted before being added to the culture medium of RAW264.7 cells.

Statistical Analysis

For all experiments ($\geq n=3$), data are expressed as the mean ± standard deviation (S.D.). One-way analysis of variance (ANOVA) and Student's t-test were performed using the data analysis tool in Microsoft Excel (WA, USA) for statistical analysis. * and **indicate $p<0.05$ and $p<0.01$, respectively.

Database

The 16 S rRNA gene sequence of strain GIF001 has been deposited in the DDBJ/EMBL/GenBank database under accession number LC907079.2. The sequence of the surface layer-associated protein (SLAP) gene is available under accession number LC907080.1.

Results

Preparation of EV-LNPs in Lactic Acid Bacteria

To produce EV-LNPs from lactic acid bacterial, different strains were isolated from commercially available supplements (Table S1). Since some species, such as *L. delbrueckii*, were difficult to isolate as single species, we used an isolated strain, NBRC 3202. Six stably propagating species were cultured in MRS medium for 24 h. For the purification of EV-LNPs, a filter-trapping method was employed (Fig. 1A). The culture medium was first filtered through a 0.1 μm PES filter, and EV-LNPs were subsequently captured using a 0.05 μm PCTE membrane. The protein and lipid membranes of the purified EV-LNPs were dual-labeled with GIF-2276 and Exo-SP Red, respectively, and then separated using an HPLC-SEC system (Fig. 1B).

The protein and lipid signal peaks were nearly identical (within ±0.2 s) across all EV-LNPs purified from different species, indicating the formation of protein–lipid complexes. DLS analysis showed that the EV-LNPs ranged in size from 30 to 100 nm (Fig. 1C), and TEM revealed a variety of nanoparticles in all EV-LNP samples (Fig. 1D). These results suggest that the morphology and size of EV-LNPs varied among lactic acid bacterial species. Since EV-LNPs from *L. helveticus* (a strain closely related to VHProbi Y21) could be purified more readily than those from other species, we chose to focus on *L. helveticus*. The concentration of the isolated *L. helveticus* EV-LNPs was 7.2×10^{10} particles/mL (Fig. S1B), corresponding to 0.5 mg protein/mL.

Fig. 1 Purification of EV-LNPs derived from lactic acid bacteria. (**A**) Schematic representation of EV-LNP purification. (**B**) HPLC-SEC analysis of EV-LNPs fluorescent-labeled with protein and lipid. Retention times of EV-LNPs peaks are indicated. (**C**) DLS analysis of EV-LNPs. Average particle sizes are shown. (**D**) TEM images of EV-LNPs

EV-LNPs Derived from *L. helveticus* Enhance Immune Responses

First, we examined whether EV-LNPs from *L. helveticus* could be incorporated into mammalian cells. EV-LNPs covalently labeled with GIF-2276 (green) were added to RAW264.7 cells whose lysosomes had been pre-labeled with LysoBright Red (Fig. 2A). The green EV-LNP signals colocalized with lysosomal signals, becoming apparent after 3 h. These observations suggest that EV-LNPs derived from *L. helveticus* are efficiently taken up by RAW264.7 cells and subsequently degraded in lysosomes. Some constituents in EV-LNPs may leak from the degradation system and potentially function independently. Because HEK293A cells (human embryonic kidney epithelial-like cells) exhibit a flat morphology that is suitable for microscopic observation, we performed the same evaluation in this cell line. Consistently, the EV-LNPs signals showed clear co-localization with lysosomes (Fig. S3A).

Since *L. helveticus* strains SBT2171 [17] and HY7801 [18] and their EV-LNPs have been reported to downregulate immune responses, we examined whether EV-LNPs derived from the present *L. helveticus* strain act as immune modulators by assessing nitric oxide (NO) production in RAW264.7 monocytes. First, we determined an appropriate pre-incubation period for *L. helveticus* EV-LNPs (Fig. S3B). A 3-h pre-incubation was sufficient to evaluate the effects of EV-LNPs on LPS-induced NO production. In the absence of LPS stimulation, EV-LNPs slightly induced NO production in unstimulated RAW264.7 cells (Fig. 2B). In contrast, EV-LNPs cooperatively enhanced NO production in the presence of LPS. When EV-LNPs–depleted fractions were prepared from the flow-through fraction (Fig. S4), these fractions did not enhance LPS-induced NO production.

The NO production correlated with increased iNOS protein levels (Fig. 2C). Similar results were obtained when the *iNos (Nos2)* promoter activity was evaluated as an indicator of immune response (Fig. 2D). Since the immune-stimulating responses might occur at the transcriptional level, other pathways were also examined using reporter assays. Transcriptional activities regulated by both AP-1 (Fig. S5A) and NF-κB (Fig. S5B) were upregulated upon the addition of EV-LNPs. Western blot analyses of NF-κB and p38 in RAW264.7 cells pretreated with *L. helveticus* EV-LNPs for

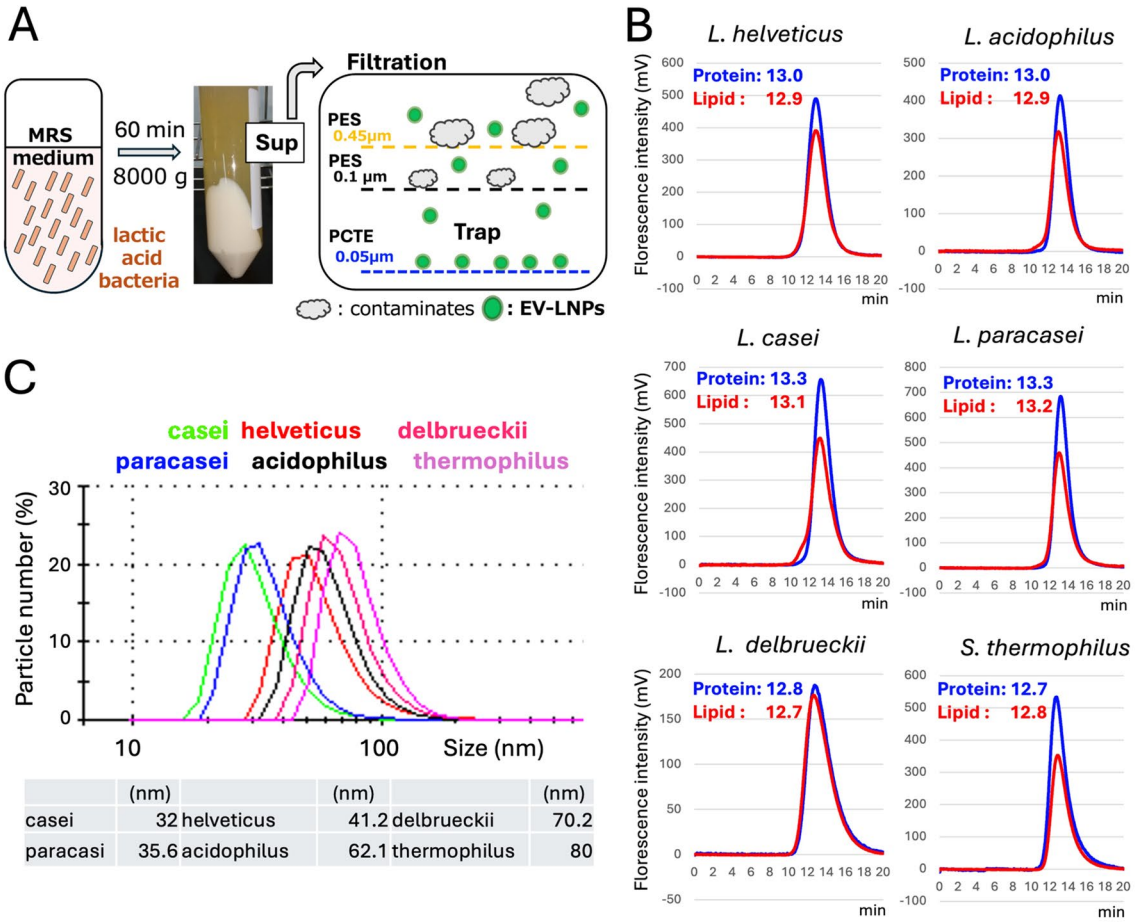

	(nm)		(nm)		(nm)
casei	32	helveticus	41.2	delbrueckii	70.2
paracasi	35.6	acidophilus	62.1	thermophilus	80

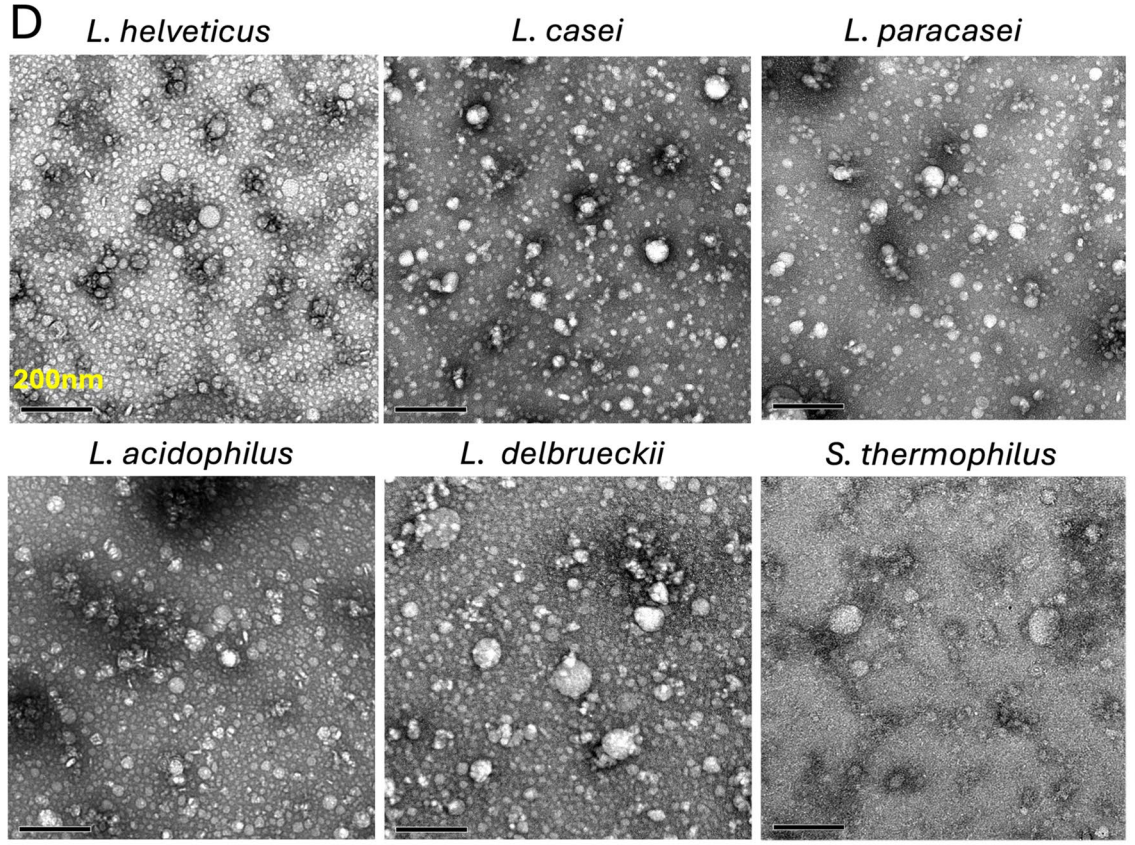

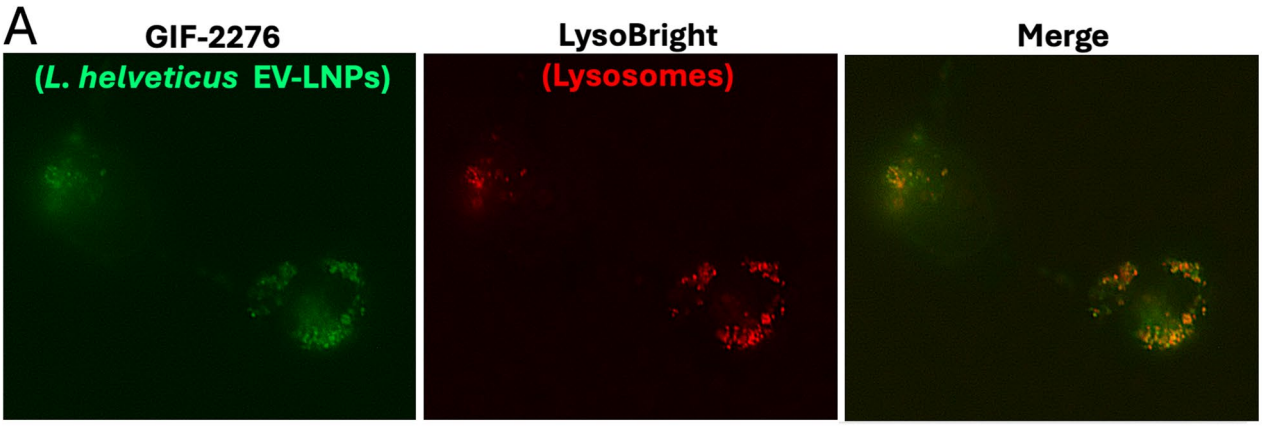
A
GIF-2276
(L. helveticus EV-LNPs)
LysoBright
(Lysosomes)
Merge

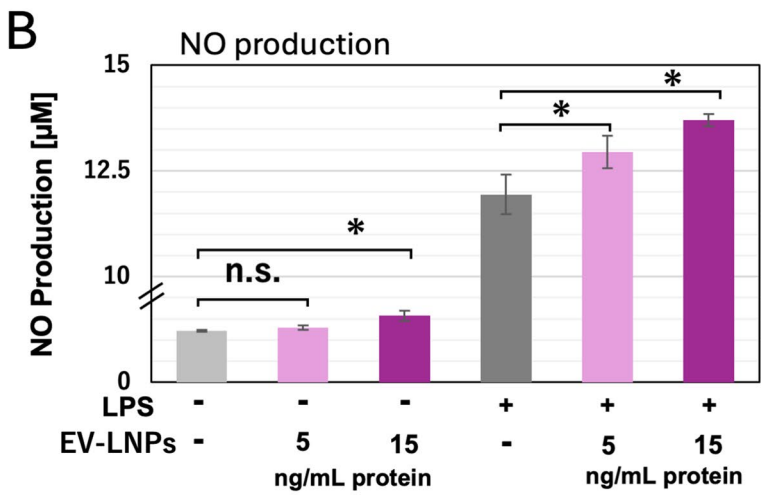
B
NO production
NO Production [μM]
15
12.5
10
0
n.s.
*
*
*
LPS - - - + + +
EV-LNPs - 5 15 - 5 15
ng/mL protein
ng/mL protein

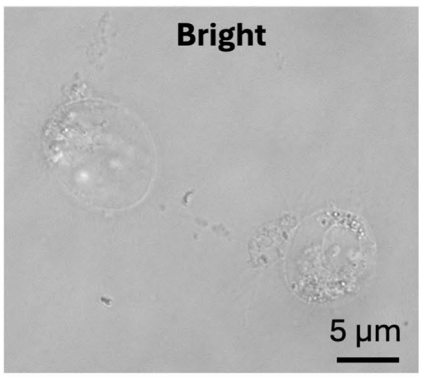
Bright
5 μm

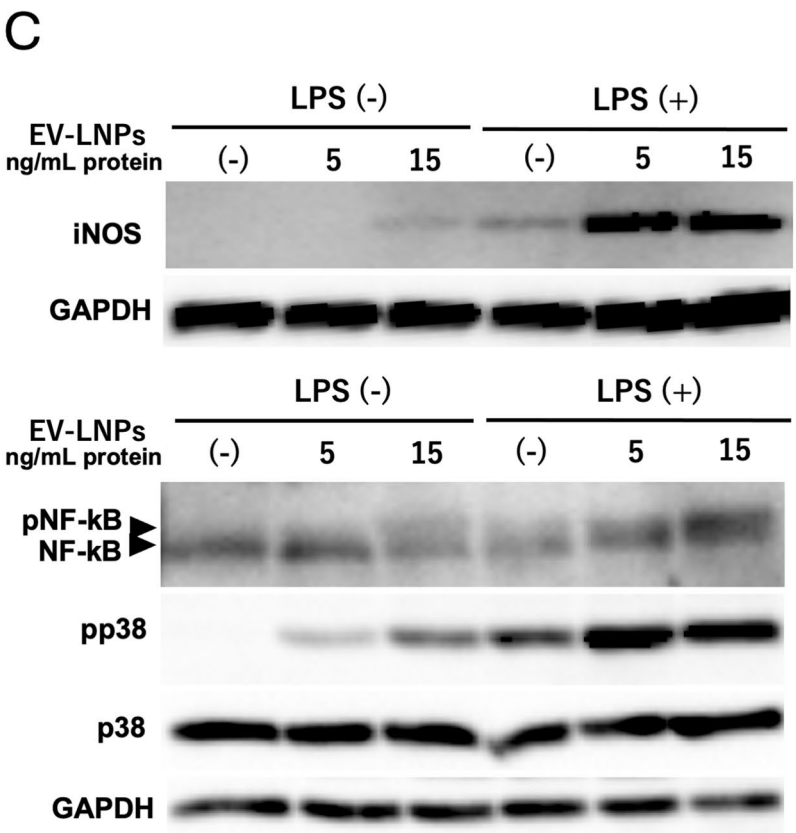
C
LPS (-)
LPS (+)
EV-LNPs
ng/mL protein
(-) 5 15 (-) 5 15
iNOS
GAPDH
LPS (-)
LPS (+)
EV-LNPs
ng/mL protein
(-) 5 15 (-) 5 15
pNF-kB
NF-kB
pp38
p38
GAPDH

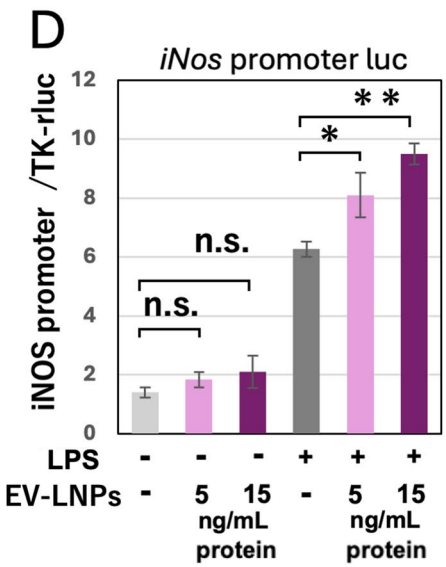
D
iNos promoter luc
iNOS promoter /TK-rluc
12
10
8
6
4
2
0
n.s.
n.s.
*
**
LPS - - - + + +
EV-LNPs - 5 15 - 5 15
ng/mL protein
ng/mL protein

Fig. 2 *L. helveticus*-derived EV-LNPs enhance immune responses. (**A**) EV-LNPs (15 ng protein) were labeled with GIF-2276 and incubated with RAW264.7 cells in 1 mL of medium for 3 h; lysosomes had been pre-labeled with LysoBright Red. (**B**) Nitric oxide (NO) production was measured in RAW264.7 cells treated with EV-LNPs in the absence or presence of 0.5 µg/mL LPS for 24 h. Means and S.D. are shown ($n = 3$). n.s., not significant; * and ** indicate $p < 0.05$ and $p < 0.01$, respectively. (**C**) Western blot analysis of iNOS protein in RAW264.7 cells after 3 h incubation with EV-LNPs, followed by 24 h stimulation with LPS (*upper set*). Western blot analysis of NF-κB, phosphorylated p38 (pp38), and total p38 proteins in RAW264.7 cells after 3 h incubation with EV-LNPs, followed by 15 min stimulation with LPS (*lower set*). (**D**) *iNos* promoter activity was measured as in (B). ($n = 3$)

3 h, followed by 15 min of LPS stimulation, suggested that the EV-LNPs induced hyperphosphorylation of both proteins (Fig. 2C). This was evidenced by band shifts for NF-κB and by enhanced reactivity with antibodies recognizing the phosphorylated form of p38. Furthermore, secretion of the pro-inflammatory cytokine IL-6 (Fig. S5A) and TNFα(Fig. S5B)was enhanced by EV-LNPs, suggesting that the present *L. helveticus* EV-LNPs have the potential to stimulate immune responses in RAW264.7 cells. These immunostimulatory activities were accompanied by enhanced transcriptional activity mediated by AP-1 and NF-κB (Fig. S5C and D).

SLAP Activates Immune Responses

To identify the molecules responsible for stimulating immune responses, proteins contained in *L. helveticus* EV-LNPs were analyzed. SDS-PAGE revealed that the protein composition varied depending on the lactic acid bacterial species (Fig. S6A). *L. helveticus* EV-LNPs contained two major proteins of approximately 47 kDa and 36 kDa (Fig. S6B), and the 47 kDa protein was specifically labeled with GIF-2276. To identify these proteins, the protein bands were subjected to proteome analyses, which revealed a SLAP and type I GAPDH (Fig. S6C). We could not identify SLAP in the EV-LNPs derived from other lactic acid bacteria.

The SLAP is a secreted, membrane-associated protein that is a typical feature of symbiotic bacteria. Therefore, an antibody against this protein was generated (Fig. S6B) and used to assess the purity of the SLAP (Fig. 3A). *L. helveticus* cells were collected by centrifugation, and the SLAP protein located on the cell membrane was extracted using 2 M LiCl, followed by dialysis, which yielded SLAP with high purity.

When RAW264.7 cells were incubated with purified SLAP for 3 h and subsequently washed with PBS, immunoreactive (SLAP) signals in RAW264.7 cells were detected in proportion to the SLAP concentration in the medium (Fig. S7A). Because the SLAP exhibited cytotoxicity at 100 ng/mL (Fig. S7B), 30 ng/mL was set as the maximum concentration in subsequent experiments. Similar to EV-LNPs, the purified SLAP enhanced NO secretion in RAW264.7 cells (Fig. 3B). Notably, SLAP induced NO secretion even without LPS stimulation, and both iNOS protein expression (Fig. 3C) and *iNos* gene promoter activity (Fig. 3D) were dependent on SLAP.

A positive correlation was observed between IL-6 (Fig. S7C), TNFα (Fig. S7D), and NO secretion in RAW264.7 cells. Reporters for AP-1-Luc (Fig. S7E) and NF-kB-Luc (Fig. S7F) also activated by the addition of the SLAP. Interestingly, AP-1-Luc activity was induced by the SLAP even in the absence of LPS, whereas NF-κB-Luc activation was primarily observed upon LPS stimulation. The phosphorylation status of p38 and NF-κB (Fig. 3C) was almost consistent with the reporter assays of AP-1-Luc and NF-κB-Luc, respectively.

To eliminate potential contamination in the EV-LNPs and SLAP fractions, we performed both a Limulus Amebocyte Lysate (LAL) assay (Fig. S8A and B). The results suggested that both the EV-LNP and SLAP fractions had endotoxin levels of ≤ 10 ng/mL LPS, as determined by the LAL assay, and that endotoxin at this concentration did not induce immune responses in RAW264.7 cells. In addition, an endotoxin neutralization assay using polymyxin B in combination with the peptide Toll-like receptor (TLR) 4 agonist RS09 (Fig. S8C) further supported the presence of negligible endotoxin levels. In contrast, the effect of the SLAP fraction on NO production in RAW264.7 cells was weakened by supplementation with the TLR2 antagonist IN-C29 (Fig. S8D), indicating that the SLAP fraction may contain TLR2-activating substances that engage the AP-1 pathway. Alternatively, it has been suggested that SLAP may enhance immune responses at high concentrations through TLR2 priming.

Overexpression of SLAP in RAW264.7 Cells Activates Immune Responses

To test whether SLAP itself could modulate TLR4 signaling in RAW264.7 cells, we conducted an artificial experiment involving intracellular SLAP overexpression (GenBank accession: LC907080.1) (Fig. S2). An expression plasmid encoding the SLAP, with humanized codons, was transfected into RAW264.7 cells, resulting in the production of immunoreactive protein (Fig. S9). Overexpression of SLAP enhanced *iNos* promoter activity in response to LPS stimulation (Fig. 4A). Although NF-κB–Luc activity was positively correlated with *iNos* promoter activity, AP-1–Luc activity remained unchanged upon SLAP overexpression (Fig. 4B). IL-6 levels in the culture medium showed a similar trend to the *iNos* and NF-κB results (Fig. 4C). These results suggest that the SLAP on EV-LNPs may enhance immune responses intracellularly in RAW264.7 cells via the NF-κB signaling

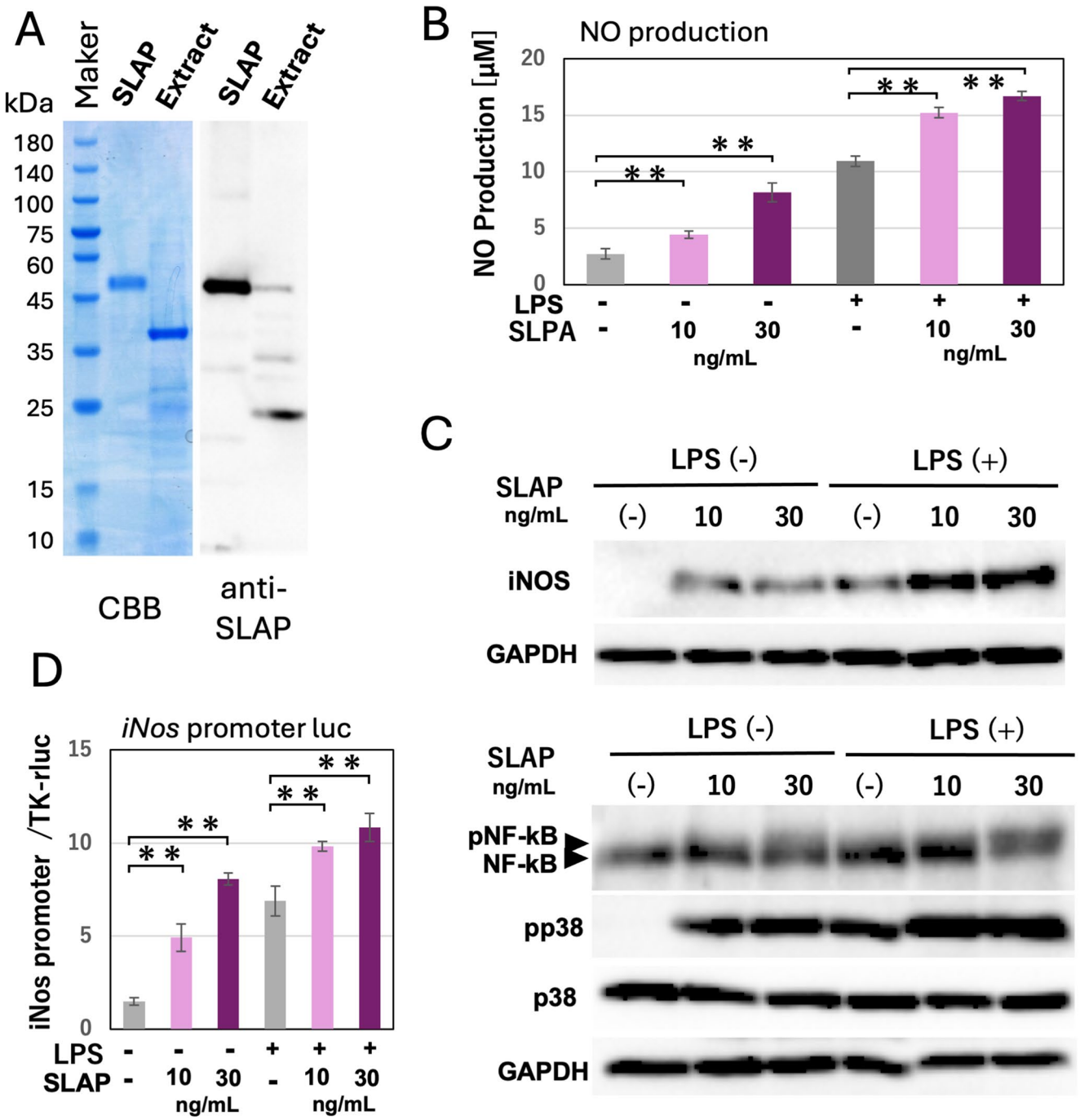

Fig. 3 *L. helveticus*-derived SLAP enhance immune responses. (**A**) Comparison between the purified SLAP and the whole cell extract of *L. helveticus* by SDS-PAGE. CBB staining and Western blotting using an anti-SLAP antibody are shown. (**B**) Nitric oxide (NO) production was measured in RAW264.7 cells treated with EV-LNPs in the absence or presence of 0.5 μg/mL LPS for 24 h. Means and S.D. are shown ($n=3$). n.s., not significant; * and ** indicate $p<0.05$ and $p<0.01$, respectively. (**C**) Western blot analysis of iNOS protein in RAW264.7 cells after 3 h incubation with EV-LNPs, followed by 24 h stimulation with LPS (*upper set*). Western blot analysis of NF-κB, phosphorylated p38 (pp38), and total p38 proteins in RAW264.7 cells after 3 h incubation with EV-LNPs, followed by 15 min stimulation with LPS (*lower set*). (**D**) *iNos (Nos2)* promoter activity were measured in RAW264.7 cells treated with the SLAP for 24 h ($n=3$)

pathway, and that the AP-1 pathway may also be activated when high levels of the SLAP or contaminants are present in the culture medium.

Next, we assessed the importance of the SLAP domain using an overexpression system (Fig. 4D). Deletion of the SLAP domain abolished the upregulation of *iNos* promoter activity. In contrast, the SLAP domain alone was sufficient to enhance *iNos* promoter activity, suggesting that the SLAP domain is essential for enhancing immune responses. However, these experiments involve forced SLAP overexpression, which does not occur naturally in mammalian cells or tissues, and thus provide only preliminary findings. Moreover, transfection efficiency differs among cell types, and the process itself is associated with inherent cytotoxicity.

L. helveticus SLAP Enhances *E. coli* Uptake in RAW264.7 Cells Via EV-LNPs

To investigate the physiological function of *L. helveticus*-derived SLAP, we evaluated *E. coli* uptake, since LPS originates from *E. coli*, as described in a previous report [15]. When RAW264.7 cells were incubated with live *E. coli* for 24 h (Fig. 5A), their morphology changed from a round to a flattened shape, and some cells exhibited dendritic structures. Quantitative analysis indicated that *L. helveticus* EV-LNPs and purified SLAP reduced the population of round-shaped cells and increased the proportion of flattened cells. This effect was enhanced by *E. coli*, especially when combined with EV-LNPs or SLAP, increasing dendritic cells.

Finally, we evaluated the uptake rate of *E. coli* by RAW264.7 cells. To enable visualization, *E. coli* was labeled with mCherry, a red fluorescent protein. When RAW264.7 cells were incubated with *E. coli* alone, 10% of the RAW264.7 cells were positive for mCherry (*E. coli*) (Fig. 5B and C). However, the addition of *L. helveticus* EV-LNPs or SLAP enhanced the accumulation of red fluorescent signals within RAW264.7 cells. Quantitative analysis (Fig. 5C) indicated that *L. helveticus* EV-LNPs or SLAP increased the number of mCherry-positive RAW264.7 cells, particularly in those exhibiting dendritic morphology. These results suggest that *L. helveticus* EV-LNPs may enhance the ability of macrophages to eliminate *E. coli* through SLAP-mediated mechanisms.

Discussion

We show that EV-LNPs of *L. helveticus* strain GIF001 are rapidly internalized by RAW264.7 cells, possibly via TLR4-independent mechanisms, because HEK293A cells lack TLR4. After internalization, EV-LNPs are degraded in lysosomes. It is possible that a portion of the degraded SLAP components, potentially including the C-terminal domain, functions as a signal or trigger that activates the phagocytic machinery in RAW264.7 cells (Fig. S10).

In lactic acid bacteria, SLAPs are widely present on the S-layer of *Lactobacillaceae*, including *L. helveticus* [5, 17–19]. They help maintain cell envelope integrity and protect against pH changes, enzymes, and detergents [20]. Mutations in the SLAP gene impair the cell division of their own bacteria. In addition, SLAPs play a key role in mediating adhesion to host epithelial surfaces, particularly in the gastrointestinal tract [7, 19]. This adhesion promotes the colonization and persistence of probiotic strains, enabling them to compete with pathogens and maintain a balanced bacterial flora [5]. During these interactions, SLAPs may also modulate the host immune system by influencing antigen-presenting cells such as dendritic cells and macrophages [21]. Through this modulation, they contribute to immune homeostasis and may help reduce inflammation and important for bacterial interaction with the extracellular environment [7, 21, 22]. These findings support the hypothesis that SLAPs may participate in intercellular communication, possibly through their association with extracellular vesicle-like structures that mediate signaling among bacteria and between bacteria and the host.

SLAPs bind noncovalently to the peptidoglycan layer beneath the S-layer in Gram-positive bacteria [22–25], ensuring stable attachment. They may also interact electrostatically with membrane-anchored lipoteichoic acids (LTA) [26], and, less frequently, with negatively charged phospholipids associated with vesicle formation. Since EV-LNPs originate from bacterial membranes, their SLAP-binding to EV-LNPs may mimic native interactions [11, 27]. LTA acts as a TLR2 agonist and can modulate TLR4 signaling through mitogen-activated protein kinase (MAPK) pathways, including p38, as well as NF-κB signaling, resulting in the induction of TNF-α, IL-6, and iNOS expression [28]. SLAP from *L. helveticus* (SBT2171 strain) has also been reported to induce β-defensin 2 expression in human colorectal adenocarcinoma–derived epithelial CaCo-2 cells via activation of the TLR2–JNK pathway [17].

However, the same strain (SBT2171) has been shown to suppress LPS-induced TLR4 signaling through activation of the TLR2/MAPK/NF-κB pathway in mouse macrophages [17, 29]. This suppressive effect is mediated by the induction of the immunoregulatory protein A20, suggesting that TLR2 signaling can act as both a positive and negative regulator of immune responses, including LPS-induced TLR4 signaling. In our experiments, the TLR2 antagonist IN-C29 partially inhibited the enhanced NO production by the SLAP fraction, suggesting that SLAP may act as a TLR2-associated priming or co-stimulatory factor, rather than functioning

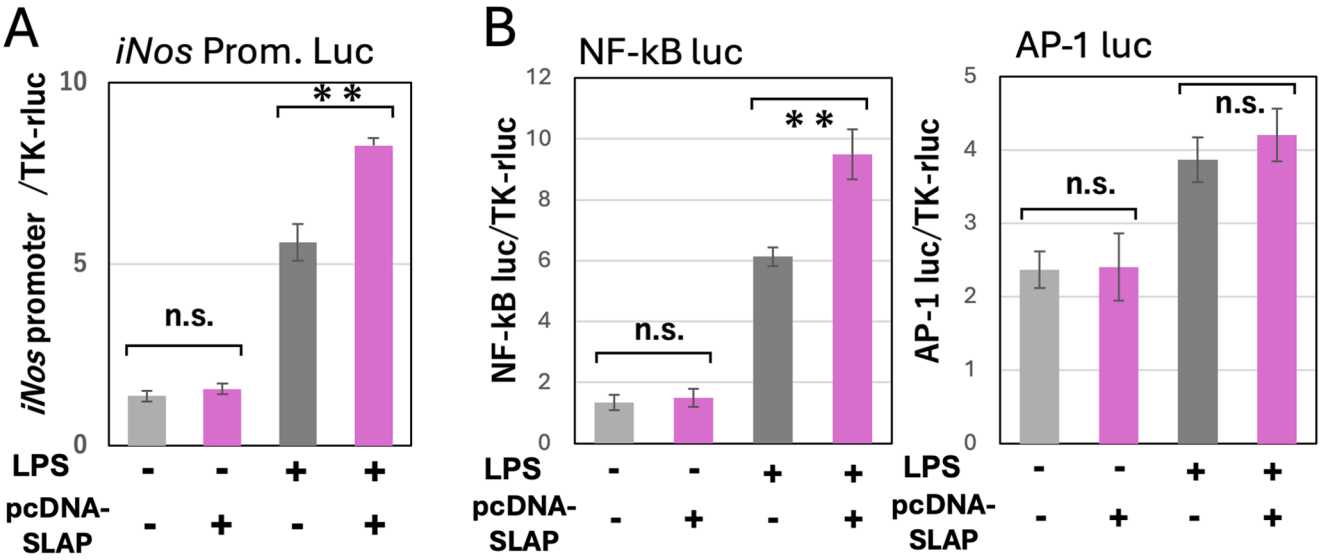
A
iNos Prom. Luc
iNos promoter /TK-rluc
10
5
0
n.s.
* *
LPS - - + +
pcDNA-SLAP - + - +
B
NF-kB luc
NF-kB luc/TK-rluc
12
10
8
6
4
2
0
n.s.
* *
LPS - - + +
pcDNA-SLAP - + - +
AP-1 luc
AP-1 luc/TK-rluc
5
4
3
2
1
0
n.s.
n.s.
LPS - - + +
pcDNA-SLAP - + - +

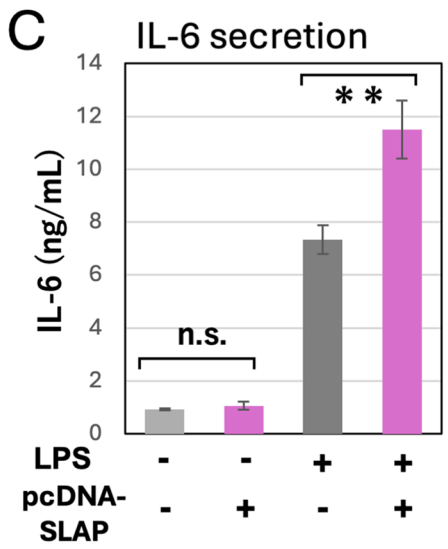
C
IL-6 secretion
IL-6 (ng/mL)
14
12
10
8
6
4
2
0
n.s.
* *
LPS - - + +
pcDNA-SLAP - + - +

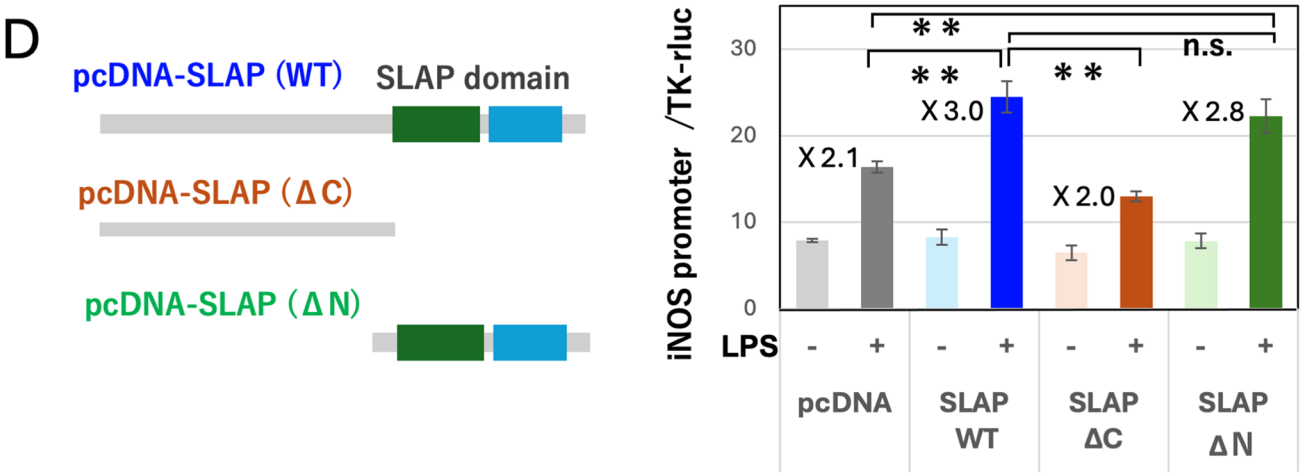
D
pcDNA-SLAP (WT)
SLAP domain
pcDNA-SLAP (ΔC)
pcDNA-SLAP (ΔN)
iNOS promoter /TK-rluc
30
20
10
0
* *
* *
* *
n.s.
X 2.1
X 3.0
X 2.0
X 2.8
LPS - + - + - + - +
pcDNA
SLAP WT
SLAP ΔC
SLAP ΔN

Fig. 4 Overexpression of SLAP in RAW264.7 cells enhances immune responses. (**A**) RAW264.7 cells were transiently transfected with an iNos promoter–driven reporter and an SLAP expression vector, and then stimulated with LPS (0.5 μg/mL) for 24 h ($n = 3$). n.s., not significant; $^{**}p < 0.01$. (**B**) NF-κB and AP-1 reporter activities were also assessed. (**C**) IL-6 levels in the culture medium were measured ($n = 3$). (**D**) Constructs encoding the SLAP domain-deleted mutant (1-325 aa) and the SLAP domain alone (326–451 aa) were generated and subjected to the *iNos* reporter assay ($n = 3$). Fold induction by LPS relative to non-stimulated cells is indicated

as a direct TLR4 agonist. On the other hand, although LTA may be present in the EV-LNP fraction, its activity was not affected by IN-C29, suggesting that the amount of LTA contained in the EV-LNPs may not be sufficient to activate TLR2 signaling.

Recent reports describe functions of EVs or EV-LNPs derived from a number of microorganisms [30]. The generation of bacteria-derived EVs is generally classified into membrane budding or the release of periplasmic material associated with cell death. The former contains peptidoglycan, whereas the latter does not. Because SLAP is a protein associated with peptidoglycan, the EV-LNPs examined in this study are likely to originate from the former pathway.

Two groups have reported EVs-like nanoparticles from *L. helveticus* [17, 18]. Both nanoparticles exhibited immune-suppressive effects through the NF-κB pathway. In addition, their average particle sizes exceeded 100 nm, suggesting that our EV-LNPs may differ from previously reported nanoparticles. These differences may have originated from variations in strain or culture conditions, such as incubation at 33–37 °C.

Intracellularly overexpressed SLAP also activates immune responses in a manner similar to EV-LNPs, and the deletion of the SLAP domain abolishes this activation, suggesting that SLAP may exert its function either after being incorporated into host cells or after being re-secreted through mechanisms such as via extracellular vesicles [31]. In this context, SLAP and EV-LNPs may serve as remote mediators through which intestinal symbiotic bacteria enhance the host defense system in response to harmful stimuli such as LPS [32]. The difference in immune-activating properties between EV-LNPs and purified SLAP is that EV-LNPs activate immune responses in an LPS-dependent manner possibly via NF-κB pathway, whereas purified SLAP activates immune responses independently of LPS, particularly through the p38/AP-1 signaling pathway. However, the possibility of contamination in the purified SLAP fraction with immune-activating substances similar to LPS cannot be exclude.

Since *E. coli* possesses LPS [5], we conducted the assay using *E. coli* together with EV-LNPs or SLAP. In the presence of *E. coli*, EV-LNPs or SLAP induced morphological changes in RAW264.7 cells and promoted bacterial uptake. These results suggest that EV-LNPs derived from *L. helveticus* may help maintain the bacterial flora, likely through SLAP-mediated interactions with host immune systems.

Moreover, it has been reported that the SLAP domain in *L. acidophilus* can be used as a tag for protein purification by taking advantage of the membrane-binding properties [8]. It should also be noted that, in this study, MRS medium was used for the production of EV-LNPs from *L. helveticus*, rather than daily food. Further elucidation of the EV-LNPs of microorganisms, as well as the industrial applications of SLAPs [12, 27], will be necessary.

Conclusion

This study demonstrates that EV-LNPs derived from *L. helveticus* strain GIF001 contain SLAP and that both EV-LNPs and SLAP enhance immune-related responses in RAW264.7 cells. SLAP promoted NO and IL-6 production, augmented NF-κB signaling in response to LPS, and increased bacterial uptake, with *iNos* synthase promoter activation dependent on the SLAP domain. Although these findings are limited to an in vitro model, they provide mechanistic insight into EV-mediated host–microbe communication and suggest a role for SLAP-associated EV-LNPs in the regulation of innate immune responses.

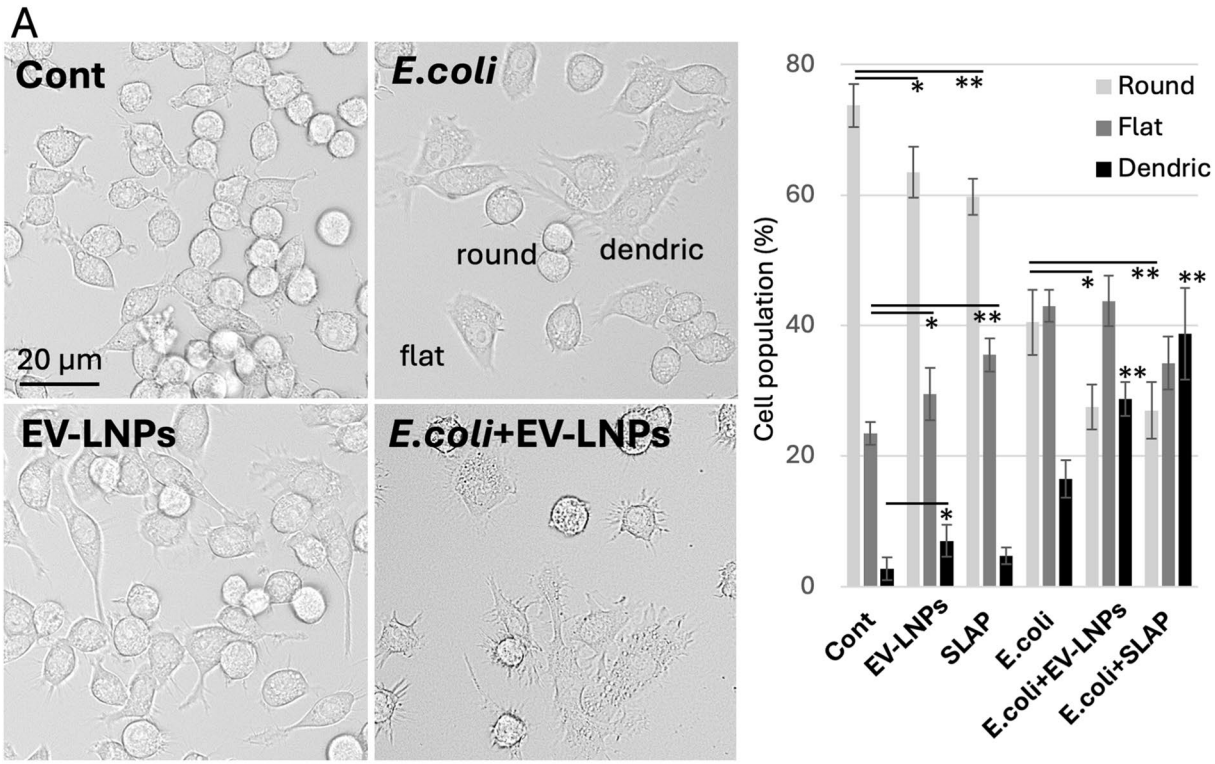
A
Cont
E.coli
round
dendric
flat
20 μm
EV-LNPs
E.coli+EV-LNPs
Cell population (%)
Round
Flat
Dendric
Cont
EV-LNPs
SLAP
E.coli
E.coli+EV-LNPs
E.coli+SLAP

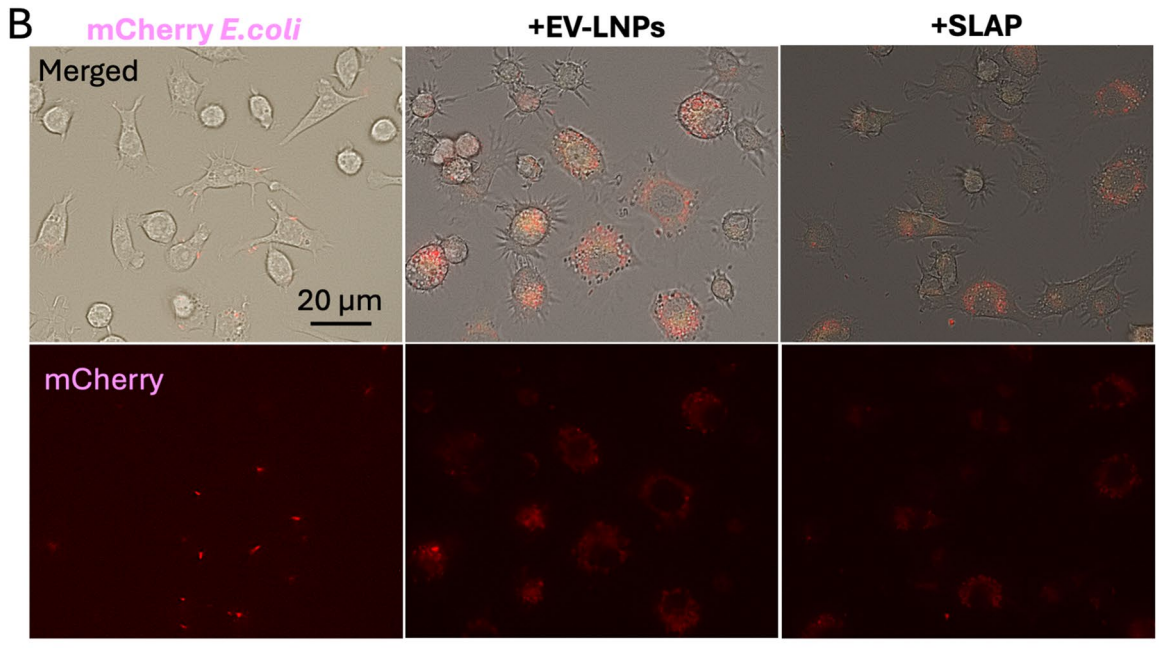
B
mCherry E.coli
+EV-LNPs
+SLAP
Merged
20 μm
mCherry

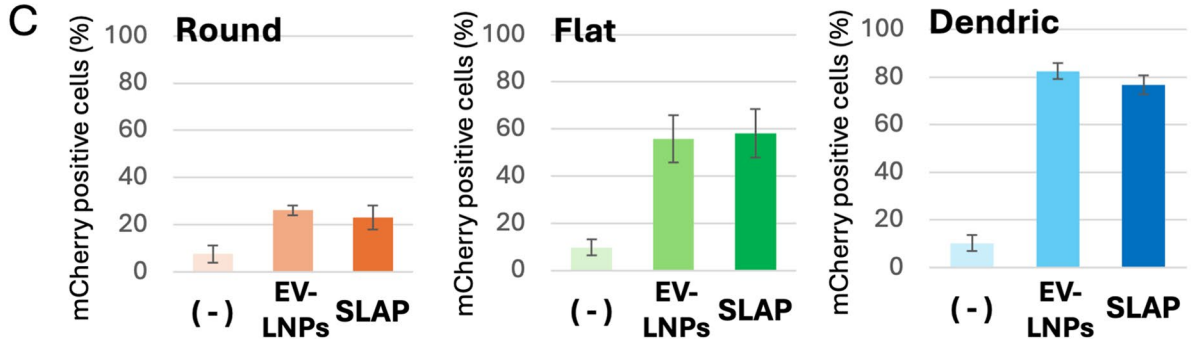
C
Round
Flat
Dendric
mCherry positive cells (%)
(-)
EV-LNPs
SLAP

Fig. 5 *L. helveticus*-derived EV-LNPs and SLAP enhance dendritic elongation and facilitate *E. coli* uptake. (**A**) Cell morphology of RAW264.7 cells incubated with live *E. coli* (5×10^5 CFU/mL) and *L. helveticus*-derived EV-LNPs (15 ng/mL, protein basis) for 24 h. The left panels show bright-field images. A representative scale bar is shown. The graph on the right shows the percentage distribution of cell morphology categories after each treatment, including treatment with 30 ng/mL SLAP, based on a count of 100 cells. Means and S.D. are shown ($n = 8$). * and ** indicate $p < 0.05$ and $p < 0.01$, respectively. (**B**) RAW264.7 cells were incubated with mCherry expressing *E. coli* for 12 h with or without EV-LNPs or SLAP. The upper panels show merged images of bright-field and red fluorescence channels. (**C**) The distribution of mCherry-positive cells, indicating uptake of *E. coli*, is shown for each morphological category. When the red signal was observed only on the cell surface, it was considered not to be incorporated by RAW264.7 cell

Supplementary Information The online version contains supplementary material available at https://doi.org/10.1007/s00284-026-04783-8.

Acknowledgements We would like to thank Dr. Kaori Tanaka (Gifu University) for giving us advise to culture lactic acid bacteria.

Funding This study is partially supported by JSPS (23K04504), Japan Dairy Association (J-milk) (2024), and Tokai Foundation for Industrial Technology Promotion (2023–2024).

Data Availability The datasets generated during and/or analyzed during the current study are available from the corresponding author on reasonable request. The DNA sequences of the 16 S ribosomal RNA gene and the *slap* gene were deposited in GenBank under the accession numbers LC907079.2 and LC907080.1, respectively.

Code Availability This study did not use any custom code.

Declarations

Conflict of interest H.T. owns shares worth USD 3,000 in Gifu Exosome Co., Ltd. K.F. and Y.M. each own shares worth USD 1,500 in Gifu Exosome Co., Ltd. The others have no conflicts of interest to declare.

Consent for Publication All authors of this study agreed to publish.

References

1. Sarasati A, Syahruddin MH, Nuryanti A, Ana ID, Barlian A et al (2023) Plant-Derived Exosome-like nanoparticles for biomedical applications and regenerative therapy. Biomedicines 11. https://doi.org/10.3390/biomedicines11041053
2. Yadav P, Debnath N, Pradhan D, Mehta PK, Kumar A et al (2025) Probiotic *Lactobacillus*-Derived Extracellular Vesicles: Insights Into Disease Prevention and Management. Mol Nutr Food Res (2025):e70013. https://doi.org/10.1002/mnfr.70013
3. Welsh JA et al (2024) Minimal information for studies of extracellular vesicles (MISEV2023): from basic to advanced approaches. J Extracell Vesicles 13:e12404. https://doi.org/10.1002/jev2.12404
4. Fagan RP, Fairweather NF (2014) Biogenesis and functions of bacterial S-layers. Nat Rev Microbiol 12(3):211–222. https://doi.org/10.1038/nrmicro3213
5. Assandri MH, Malamud M, Trejo FM, Serradell MLA (2023) S-layer proteins as immune players: Tales from pathogenic and non-pathogenic bacteria. Curr Res Microb Sci 4:100187. https://doi.org/10.1016/j.crmicr.2023.100187
6. Hahn MJ, Kim KK, Kim I, Chang WH (1993) Cloning and sequence analysis of the gene encoding the crystalline surface layer protein of rickettsia Typhi. Gene 133(2):129–133. https://doi.org/10.1016/0378-1119(93)90237-w
7. Liu Z, Shen T, Zhang P, Ma Y, Qin H (2011) *Lactobacillus plantarum* surface layer adhesive protein protects intestinal epithelial cells against tight junction injury induced by enteropathogenic *Escherichia coli*. Mol Biol Rep 38(6):3471–3480. https://doi.org/10.1007/s11033-010-0457-8
8. Zheng Y, Zhao J, Nie X, Chitrakar B, Gao J, Sang Y (2024) Mutual adhesion of *Lactobacillus* spp. To intestinal cells: A review of perspectives on surface layer proteins and cell surface receptors. Int J Biol Macromol 282:137031. https://doi.org/10.1016/j.ijbiomac.2024.137031
9. Furukawa S, Kawaguchi K, Chikama K, Yamada R, Kamatari YO et al (2024) Simple methods for measuring milk exosomes using fluorescent compound GIF-2250/2276. Biochem Biophys Res Commun 696:149505. https://doi.org/10.1016/j.bbrc.2024.149505
10. Sakurai A, Egashira K, Kizaki R, Sholihah AI, Koyama H et al (2025) Extracellular Vesicle-Like Nanoparticles, artificially created by heat treatment of *Euglena gracilis*, exhibit autofluorescence and suppress IL-6 expression in RAW264.7 cells. BioNanoScience 15(2):271–277. https://doi.org/10.1007/s12668-025-01887-6
11. Chikama K, Terada K, Yamamoto C, Yamamoto M, Hojo A, Fujioka K et al (2025) Extracellular Vesicle-Like nanoparticles present in fermented botanical products suppress fat absorption in the gut. J Food Sci 90:e70518. https://doi.org/10.1111/1750-3841.70518
12. Muruaga EJ, Uriza PJ, Eckert GAK, Pepe MV, Duarte CM et al (2023) Adaptation of the binding domain of *Lactobacillus acidophilus* S-layer protein as a molecular Tag for affinity chromatography development. Front Microbiol 14. https://doi.org/10.3389/fmicb.2023.1210898
13. Maeda M, Suzuki M, Fuchino H, Tanaka N, Kobayashi T et al (2022) Diversity of *Adenostemma lavenia*, multi-potential herbs, and its Kaurenoic acid composition between Japan and Taiwan. J Nat Med 76:132–143. https://doi.org/10.1007/s11418-021-01565-3
14. Kobayashi T, Tanaka N, Suzuki M, Maeda M, Batubara I et al (2022) Adenostemmoic acid B suppresses NO production by downregulating the expression and inhibiting the enzymatic activity of iNOS. Phytochem Lett 49:131–137. https://doi.org/10.1016/j.phytol.2022.03.02
15. Groesdonk HV, Schlottmann S, Richter F, Georgieff M, Senftleben U (2006) *Escherichia coli* prevents phagocytosis-induced death of macrophages via classical NF-kappaB signaling, a link to T-cell activation. Infect Immun 74:5989–6000. https://doi.org/10.1128/iai.00138-06
16. Kawaguchi K, Watanabe M, Furukawa S, Koga K, Kanamori H et al (2023) Intermittent Inhibition of FYVE finger-containing phosphoinositide kinase induces melanosome degradation in B16F10 melanoma cells. Mol Biol Rep 50:5917–5930. https://doi.org/10.1007/s11033-023-08536-9
17. Kawano M, Miyoshi M, Miyazaki T (2019) *Lactobacillus helveticus* SBT2171 induces A20 expression via toll-like receptor 2 signaling and inhibits the lipopolysaccharide-induced activation of nuclear factor-kappa b and mitogen-activated protein kinases in peritoneal macrophages. Front Immunol 10:845. https://doi.org/10.3389/fimmu.2019.00845

18. Kim H, Gwon H, Jeong JW, Kim JY, Shim JJ, Lee JH (2025) A mechanistic study of *Lactobacillus helveticus* HY7801 and its extracellular vesicles in premenstrual syndrome: role of gut microbiota and hormonal modulation. J Microbiol Biotechnol 35:e2507014. https://doi.org/10.4014/jmb.2507.07014
19. Waśko A, Polak-Berecka M, Kuzdraliński A, Skrzypek T (2014) Variability of S-layer proteins in *Lactobacillus helveticus* strains. Anaerobe 25:53–60. https://doi.org/10.1016/j.anaerobe.2013.11.004
20. de Jesus LCL, Drumond MM, Aburjaile FF, Sousa TJ et al (2021) Probiogenomics of Lactobacillus delbrueckii subsp. Lactis CIDCA 133: in Silico, in Vitro, and in vivo approaches. Microorganisms 9. https://doi.org/10.3390/microorganisms9040829
21. Klotz C, Goh YJ, O'Flaherty S, Johnson B, Barrangou R (2020) Deletion of S-Layer associated Ig-Like domain protein disrupts the *Lactobacillus acidophilus* cell surface. Front Microbiol 11:345. https://doi.org/10.3389/fmicb.2020.00345
22. Wakai T, Kano C, Karsens H, Kok J, Yamamoto N (2021) Functional role of surface layer proteins of *Lactobacillus acidophilus* L-92 in stress tolerance and binding to host cell proteins. Biosci Microbiota Food Health 40:33–42. https://doi.org/10.12938/bmfh.2020-005
23. Cheung KCP, Jiao M, Xingxuan C, Wei J (2022) Extracellular vesicles derived from host and gut microbiota as promising nanocarriers for targeted therapy in osteoporosis and osteoarthritis. Front Pharmacol 13:1051134. https://doi.org/10.3389/fphar.2022.1051134
24. Qian D, Xu P, Wang X, Du C, Zhao X, Xu J (2025) Bacterial extracellular vesicles for gut microbiome-host communication and drug development. Acta Pharmaceutica Sinica B (2025): https://doi.org/10.1016/j.apsb.2025.03.008
25. Smit E, Oling F, Demel R, Martinez B, Pouwels PH (2001) The S-layer protein of *Lactobacillus acidophilus* ATCC 4356: identification and characterisation of domains responsible for S-protein assembly and cell wall binding. J Mol Biol 305:245–257. https://doi.org/10.1006/jmbi.2000.4258
26. Bönisch E, Oh YJ, Anzengruber J, Hager FF, López-Guzmán A et al (2018) Lipoteichoic acid mediates binding of a *Lactobacillus* S-layer protein. Glycobiology 28:148–158. https://doi.org/10.1093/glycob/cwx102
27. Luo G, Yang Q, Yao B, Tian Y, Hou R et al (2019) Slp-coated liposomes for drug delivery and biomedical applications: potential and challenges. Int J Nanomed 14:1359–1383. https://doi.org/10.2147/ijn.s189935
28. Jeon H, Oh S, Kum E, Seo S, Park S, Kim G (2022) Immunomodulatory effects of an aqueous extract of black radish on mouse macrophages via the TLR2/4-mediated signaling pathway. Pharmaceuticals (Basel) 15:1376. https://doi.org/10.3390/ph15111376
29. Zhang X, Li Y, Wang Y et al (2021) Clostridium Butyricum supernatant regulates the expression of RORγt in HCT-116 cells by inhibiting the TLR2/MyD88/NF-κB signaling pathway. Curr Microbiol 78:2507–2516. https://doi.org/10.1007/s00284-021-02392-1
30. Li M, Mao B, Tang X, Zhang Q, Zhao J, Chen W, Cui S (2024) Lactic acid bacteria derived extracellular vesicles: emerging bioactive nanoparticles in modulating host health. Gut Microbes 16:2427311. https://doi.org/10.1080/19490976.2024.2427311
31. Yamada R, Michimae M, Hamamoto A, Takemori H (2024) Melanin-concentrating hormone receptor 1 is discarded by exosomes after internalization. Biochem Biophys Res Commun 710:149917. https://doi.org/10.1016/j.bbrc.2024.149917
32. Malamud M, Carasi P, Assandri MH, Freire T, Lepenies B, Serradell M (2019) S-Layer glycoprotein from *Lactobacillus Kefiri* exerts its immunostimulatory activity through glycan recognition by mincle. Front Immunol 10:1422. https://doi.org/10.3389/fimmu.2019.01422